Hindawi
International Transactions on Electrical Energy Systems
Volume 2023, Article ID 9791037, 1 page
https://doi.org/10.1155/2023/9791037

Retraction

Retracted: Model-Predicted Control System for the Real-Time Operation of an Urban Drainage System to Mitigate Urban Flood Risk: A Case Study in the Liede River Catchment, Guangzhou, China

International Transactions on Electrical Energy Systems

Received 12 December 2023; Accepted 12 December 2023; Published 13 December 2023

This article has been retracted by Hindawi, as publisher, following an investigation undertaken by the publisher [1]. This investigation has uncovered evidence of systematic manipulation of the publication and peer-review process. We cannot, therefore, vouch for the reliability or integrity of this article.

Please note that this notice is intended solely to alert readers that the peer-review process of this article has been compromised.

Wiley and Hindawi regret that the usual quality checks did not identify these issues before publication and have since put additional measures in place to safeguard research integrity.

We wish to credit our Research Integrity and Research Publishing teams and anonymous and named external researchers and research integrity experts for contributing to this investigation.

The corresponding author, as the representative of all authors, has been given the opportunity to register their agreement or disagreement to this retraction. We have kept a record of any response received.

References

[1] X. Quan, Z. Chen, T. Jiang, W. Liu, Y. Mo, and B. Chen, "Model-Predicted Control System for the Real-Time Operation of an Urban Drainage System to Mitigate Urban Flood Risk: A Case Study in the Liede River Catchment, Guangzhou, China," *International Transactions on Electrical Energy Systems*, vol. 2022, Article ID 8199192, 20 pages, 2022.

Hindawi
International Transactions on Electrical Energy Systems
Volume 2022, Article ID 8199192, 20 pages
https://doi.org/10.1155/2022/8199192

Research Article

Model-Predicted Control System for the Real-Time Operation of an Urban Drainage System to Mitigate Urban Flood Risk: A Case Study in the Liede River Catchment, Guangzhou, China

Xing Quan,[1] Zhile Chen,[1] Tao Jiang,[2] Weifei Liu,[1] Yaojun Mo,[1] and Bing Chen[1]

[1]*School of Environment and Energy, South China University of Technology, Guangzhou, Guangdong 510640, China*
[2]*School of Materials Science and Engineering, South China University of Technology, Guangzhou 510640, Guangdong, China*

Correspondence should be addressed to Bing Chen; chenbing@zcmu.edu.cn

Received 25 June 2022; Revised 12 August 2022; Accepted 25 August 2022; Published 11 October 2022

Academic Editor: Raghavan Dhanasekaran

A model-predicted control (MPC) system, which is based on a storm water management model (SWMM) and uses a multi-objective particle swarm optimization algorithm, is developed and applied to optimize the real-time operation of an urban drainage system (UDS) in the Liede River catchment, Guangzhou, China. By comparing the results of three control scenarios (i.e., the original control scenario, the current MPC, and the ideal MPC) under three typical rainfall events, the results demonstrate that the MPC system can effectively mitigate urban flood risk in engineering applications and the decision-making of the MPC system is valid. By comparing the control results of the MPC system under different rainfall return periods (e.g., 1, 2, 3, 5, and 10 years), it is found that compared with the original control scenario, the total overflow is reduced by 10%, the total overflow time is reduced by 10%, or the node overflow start time is delayed by an average of 10 minutes, and the real-time control of the MPC system is only effective when the return period of the rainfall is less than three years. It is important to explore different ways of combining the MPC system and feasible capital measures to cope with urban flood risk and challenges of climate change in future works (e.g., mean sea level rise and intense rainfall).

1. Introduction

Urban flood appears to be one of the major life- and property-threatening challenges for humans worldwide [1–3]. Many factors, such as climate change, urbanization, and the aging of drainage systems, contribute to urban flooding [4–7]. Capital measures (e.g., urban drainage system rehabilitation) and adaptive measures (e.g., detention tanks [DT] and low-impact development [LID] control) are effective for urban flood risk mitigation [8–10]. For example, Koudelak and West [11] analyzed the local urban drainage system (UDS) condition using Storm Water Management Model 5.0 (SWMM5.0) and InfoWorks CS to support the upgrading of local UDS to cope with continuous urban flood events and pollution. Yazdi et al. [12] integrated the copula method, Monte Carlo simulation (MCS), multi-objective evolutionary algorithm (EA), and hydro-dynamic models for UDS reconstruction in order to tackle floods arising from rainfall uncertainties [12]. Based on SWMM and modified particle swarm optimization (PSO), Li et al. and Duan et al. explored the effectiveness of detention tank (DT) and low-impact development (LID) measures in managing urban flood and water quality and then analyzed the uncertainty of those models. They reported that both DT alone and the combination of DT and LID could effectively control urban floods and reduce flood nodes. Relative to DT alone, LID might be more appropriate because it can reduce more flood nodes and pollution [13–16]. These evaluations suggest that the small hydropower (SHP) development in UDS is feasible and the implementation of DT measures can effectively reduce the urban flood risk and consistently generate electricity through SHP [17]. In the context of climate change, Hellmers et al. [18] evaluated how SUDS measures (e.g., infiltration, retention, and storage devices) could

mitigate flood risk under different future land-use scenarios [18]. To address the uncertainty of future flood risk, Babovic and Mijic [19] proposed the application of the adaptation tipping points (ATP) in the process of developing adaptive strategies and provided a structured approach for long-term UDS planning. Nevertheless, capital measures might not be feasible in some cases because of the high cost and long implementation time [20].

Adaptive measures should be analyzed by comparing the achieved goals against the associated costs because such measures might be unfit for cities/regions with a high-density of buildings and populations [16,20]. In such cities/regions, effective management of existing infrastructure might be a desirable alternative. This can be achieved through real-time control technology. The model-predicted control (MPC) is a widely used real-time control technology for reducing combined sewer overflows and flood events in UDS [21–24]. For example, some previous studies applied a linear controller linked with the SWMM model to optimize flood levels [25–27]. However, the implementation of a linear real-time controller might not always guarantee the best control scheme for each real-time decision. Some recent studies have examined the ability of an MPC technology (based on SWMM and evolutionary algorithms) to mitigate urban flood risk in real time and confirmed that it can provide more accurate real-time control strategies compared to a linear controller [20]. For example, based on SWMM and genetic algorithm (EA), AbouRjeily et al. [28] applied a high-performance computer (HPC; which was configured as Xeon ® e5-2670 V3 processors with a total of 60 parallel computing cores at Lille University) to compute the MPC system and control UDS in order to mitigate flooding. That study reported that the model performance was stable and the applied algorithm was robust. Based on SWMM and PSO, Jafari et al. [29] divided an MPC model into two sub-models, namely, the upstream and downstream sub-models. The upstream sub-model contained complex and considerable pipelines, but its computation results were stable and had little influence on the downstream sub-model, whereas the downstream sub-model contained few pipelines but it included all UDS actuators. Thus, the upstream sub-model operated only once, while the downstream sub-model iterated an adequate number of times in a decision period. This approach ensured the output result of the MPC system was stable and cut the computational time of the MPC system by approximately 11 minutes. Relative to the original policy, the implementation of an MPC cut the peak water-level violation from the target water level by 32.25% and decreased the number of pump switches by 28.5% [29]. Sadlera et al. [30] applied three types of servers (personal computers, HPCs, and cloud-based computers) to run a simulated MPC system for minimizing flood risk caused by intense storms and sea level rise. That study suggested that having a target water level of a storage unit and tidal boundary conditions in UDS would reduce the flood risk by 74% (compared to a passive scenario or rule-based control). That study also confirmed that the HPC and cloud computing can reduce the computation time of the MPC system greatly, whereas the cloud-based computer, such as Amazon web services (AWS), was recommended because of its low cost, flexible computation demands, and free from cyber-attacks [30]. While these studies demonstrated the effectiveness of the MPC system in reducing flood risk, they were based on historical or simulated rainfall data. In a sense, those outcomes reflected the ideal effect of the MPC system [28–30]. With the development of industrialization, the distribution of urban drainage systems has become more and more complex, and flood risk has become more and more unpredictable. Previous studies still have some limitations in this regard.

Thus, this study develops an MPC system (involving a functional human interface) using SWMM and evolutionary algorithms (PSO algorithm) to optimize the real-time operation of UDS gates in a real system in the Liede River catchment, Guangzhou, China. The aim is to investigate the application effect and evaluate the developed MPC system in a real system. First, we evaluate the application effect of the MPC system by comparing the results of three control scenarios during three different typical rainfall events (i.e., the original control scenario, the real MPC, and the ideal MPC), and examine the efficiency of the decision-making of the MPC system in practical application. The model predictive control system using the multi-objective particle swarm optimization algorithm in this article can put forward new ideas for urban flood control measures and can also provide a new direction for research on the application value of the multi-objective particle swarm optimization algorithm. To further examine the effectiveness of the MPC system, we analyze the control results of the original control scenario and the ideal MPC under different rainfall return periods (e.g., 1, 2, 3, 5, and 10 years). This article is organized as follows. Section 2 describes the methods and materials of this study. Section 3 presents the construction of real-time monitoring and control system networks. Section 4 shows the result and discussion of the application of the MPC system. The final section summarizes and concludes the application of the MPC system and puts forward potential for future work.

2. Materials and Methods

2.1. Study Area. The study area, the Liede River catchment (16.2 km^2; 113°19′–113°20′E and 23°06′–23°09′N; Figure 1), is located in the Tianhe District of Guangzhou city, China. It has a total length of about 4.3 kilometers and is an important regional location. It is the only watershed in Tianhe District that flows through the central business district of Zhujiang, New Town. In recent years, Guangzhou city has been frequently affected by flooding due to climate change, urbanization, and the aging of drainage networks [31]. It has caused great inconvenience to people's travels, and seriously affected people's daily life and drinking water safety. The frequent occurrence of waterlogging also affected many buildings and caused a lot of property losses. Statistical reports suggested that from 1980 to 2010, the number of flood events in the city increased from 7 to 113, which seriously threatened lives and properties [32]. Located in the central area of Tianhe district, Guangzhou city, the Liede River catchment is the most frequent and serious area

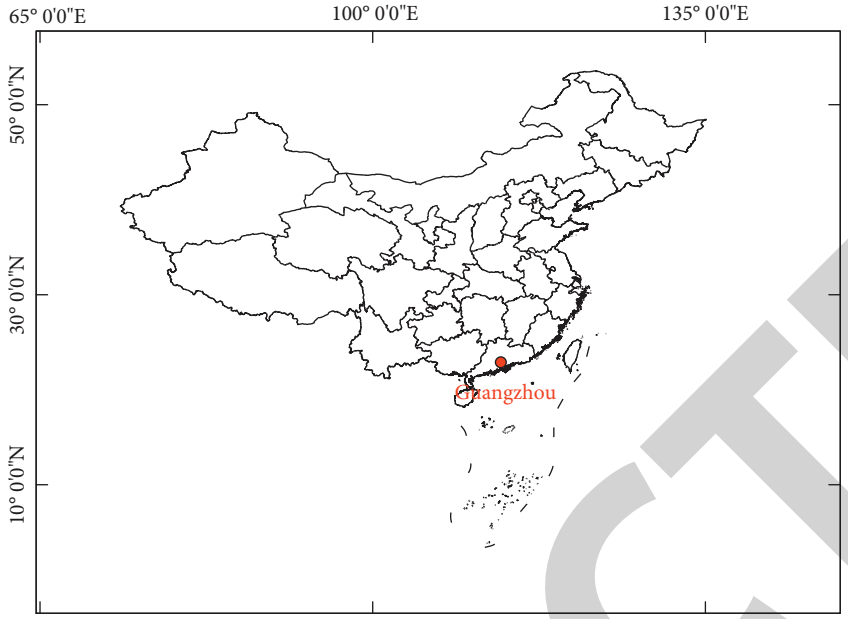

(a)

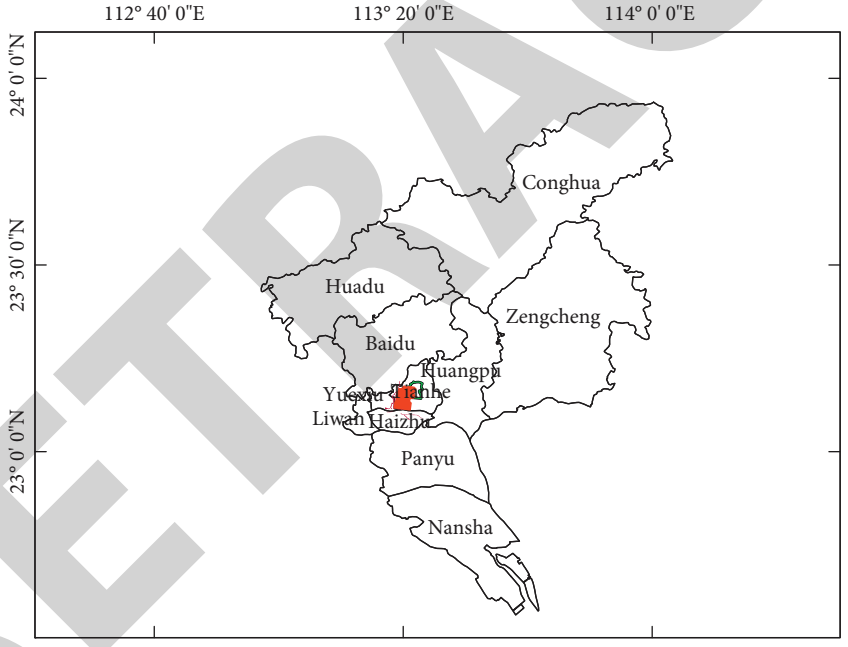

(b)

Figure 1: Continued.

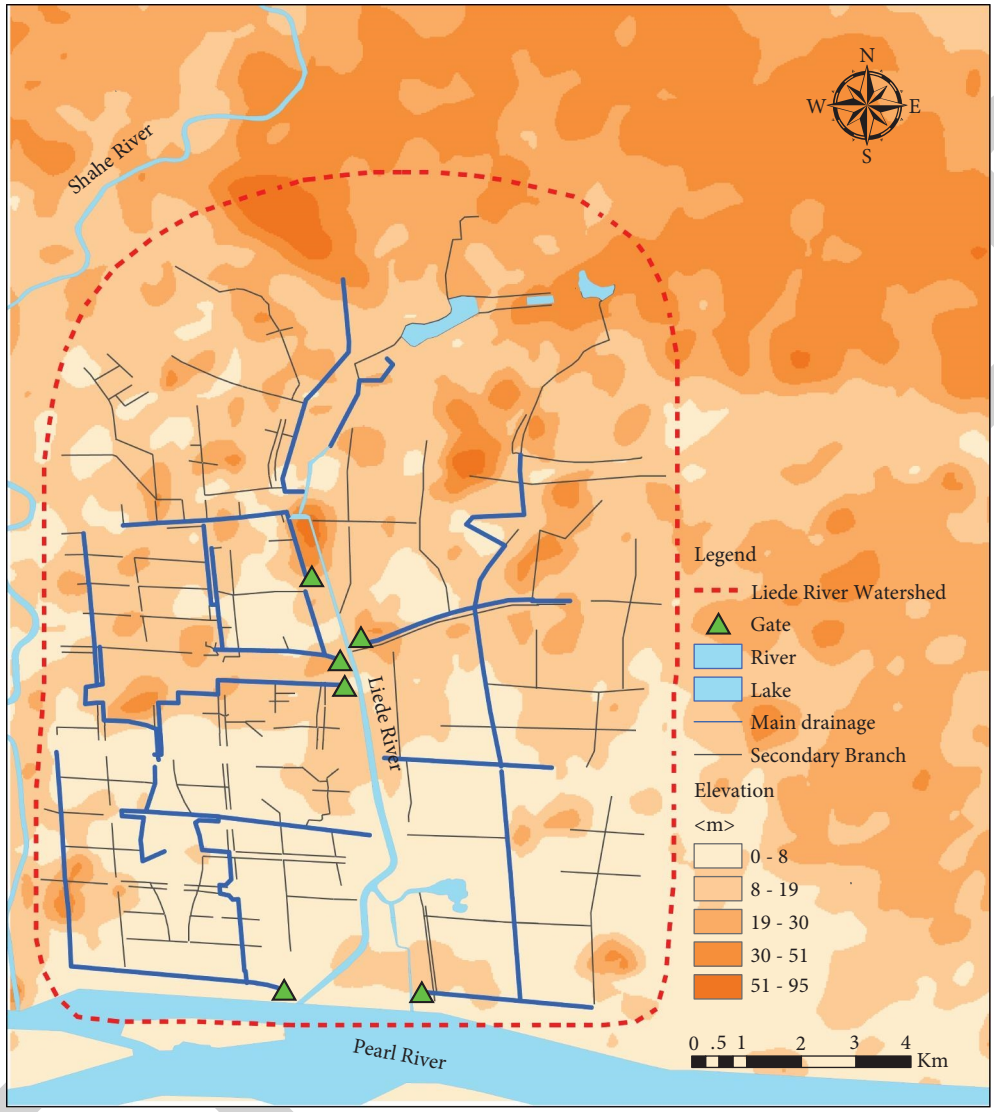

(c)

Figure 1: Study area. (a) Location of Guangzhou City in China, (b) location of the Liede River Basin in Tianhe District of Guangzhou City, and (c) Liede River catchment.

threatened by urban floods in Guangzhou city. The causes of flooding in the Liede River catchment include natural and man-made causes. Natural causes involve the intensification of extreme weather conditions driven by climate change and the river level rise caused by the characteristics of the river (e.g., low elevation, narrow channel, and shallow riverbed in the river's downstream area). These characteristics limit the drainage into the downstream river. Man-made causes include the population surge, the rise in impervious areas due to urbanization, low design capacity of UDS, and inadequate maintenance of UDS. We note that some problems occurred in the original construction process of UDS in the study catchment, such as staggered connections, and mixed connections among some drainage pipelines in UDS. To better reflect the actual conditions of the study catchment, some adjustments have been made to the boundaries of the catchment and sub-catchments (see Figure 1).

2.2. Structure of the MPC System. The MPC system consisted of field devices, a cloud database backend, and application software (see Figure 2). It is realized by establishing the model of the optimization problem and solving the optimization problem to obtain the output of the controller. Field devices included sensors and actuators, a remote terminal unit (RTU), and a transmitter. Sensors, such as water-level gauges, rain gauges, and flow meters, were used to collect field data. Actuators (sluice gates, pumps, valves, etc.) were applied to control UDS. The RTU is a data acquisition and control unit which is mainly used to collect and upload the heterogeneous sensors' data and execute the control commands issued by the application software. It consists of operating systems, monitoring software, and functional application software, and can reasonably allocate CPU time among different tasks according to the priority of each task. The

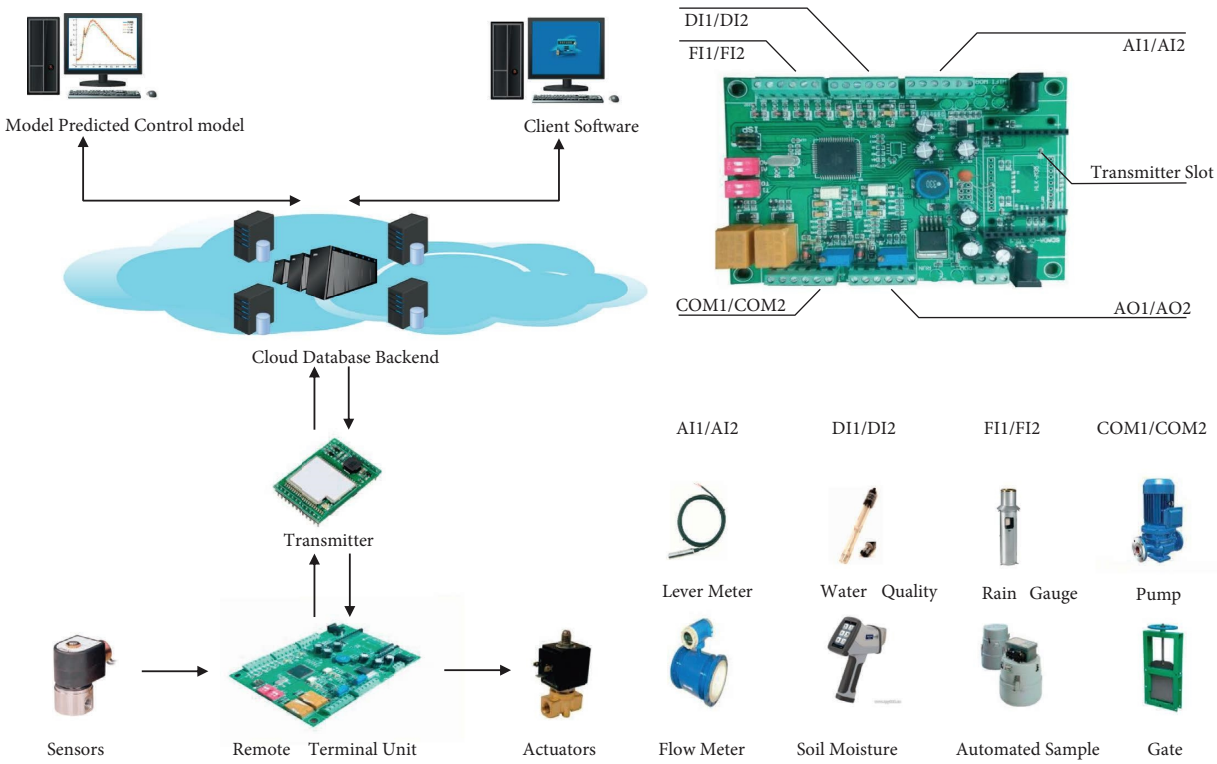

Figure 2: The MPC system. The left panel shows the structure of the MPC system, and the right panel shows the RTU and the sensors and actuators connected to each interface in the RTU.

transmitter was a wireless network transceiver that used the General Packet Radio Service (GPRS) wireless network to realize the communication between the field devices and the cloud database backend. The database backend adopted the PostgreSQL 9.2 (continuously updated open-source software; https://52north.org/) [33]. The application software included two parts, namely, client software and the MPC model, which communicated with the database back-end directly. The TCP/IP protocol was applied as the communication protocol in this system. The database backend, client software, and the MPC model were all deployed on a cloud-based computer, which was configured as Xeon ® Intel Xeon e5-2699 V5 processors with a total of 32 parallel computing cores and provided by the Aliyun Computer Company.

2.3. Client Software. Client software consisted of a front-end website and a mobile application. The front-end website used the react framework and was written in the IIS + ASP language; while the mobile application applied the Mina framework and was coded in the Java language. Client software contained the following four functions. Figure 3 shows the main interface of the front website and the mobile application:

(i) Real-time data, such as sensors and actuators data (e.g., rainfall precipitation, water level, and gate-opening ratio) and status data of field devices were viewed (e.g., battery power status and signal intensity of communication networks).

(ii) Field devices were configured and maintained, such as the configuration of field devices and the replacement of damaged field sensors and RTU.

(iii) *Real Time Alert.* Historical data collected in the system over a long period of time were analyzed through predictive analytics to create flood-related trends, and users were notified in real time once a state of emergency is reached. For example, when a public emergency occurred, users would be notified about the urban flood inundation.

(iv) *Manual Control.* The manual control could be used for sensor and actuator maintenance and emergency. The manual control is superior to the MPC system control.

2.4. MPC Model

2.4.1. Objective Functions and Boundary Condition. To reduce the adverse impact of urban floods, three objective functions were adopted in the MPC system, namely, minimum total overflow, minimum total overflow time, and maximum average overflow start time. The maximum average overflow start time is targeted to gain sufficient time for the deployment and prevent flood inundation. The gate-opening ratio was provided with 0, 10, 20, . . ., 90, 100% possibilities.

Figure 3: Real-time data interface in the front-end website and manual control interface in the mobile application.

$$\text{Min: } \left\{ W = \sum_{j=1}^{J} \sum_{t=1}^{T} X_{it} \right\}, \tag{1}$$

$$Min: \left\{ \Delta T = \sum_{j=1}^{J} \sum_{t=1}^{T} \Delta t_{it} \right\}, \tag{2}$$

$$\text{Max: } \left\{ \sum_{j=1}^{J} \frac{T_{i\text{Start}}}{J} \right\}. \tag{3}$$

In Equations (1)–(3), W is the total overflow of watershed nodes, m^3; ΔT is the total overflow time, min; J is the number of overflow nodes, T is the entire time period of a rainfall event, min; X_{it} is the overflow flow of the ith node at t time period, m^3; Δt_{it} is the overflow time of the ith node at t time period, min; and $T_{i\text{Start}}$ is the start time of overflow at the ith node, hh: mm: ss.

In the MPC model, the boundary condition was set as the water level of the outer river outside the outfall. The water level of the outer river was affected by the tide in this study, which occurred irregularly. Due to the tidal forces of the Moon and Sun on the oceans, there are two high tides and low tides that occurred on a lunar day and were often affected by extreme storms (e.g., large typhoons). Therefore, the water-level data of the boundary condition were obtained from the real-time monitoring system (see Section 3).

2.4.2. UDS Model. The UDS model is a one-dimensional model established by the SWMM. SWMM is an open-resource dynamic rainfall-runoff simulation model, developed by the Environmental Protection Agency, United States (US-EPA), which is used for urban storm event management worldwide [34, 35]. The data resources for the establishment of the UDS model included the field inspection, maintenance, and supplementary measurement data of UDS (provided by Guangzhou Sewage Treatment Co., Ltd.), original computer-aided design (CAD) of UDS (sourced from the Guangzhou Municipal Engineering Design & Research Institute), a digital elevation map (downloaded from Google Earth), land-use data (obtained from the Guangzhou Land and Resources Bureau), and the tables in the appendices of the SWMM manual. The dynamic wave was selected as its path simulation, and the simulation time step was set to 1 minute. The water-level data of nodes J5, J35, and J41 (i.e., the nodes of twelve consecutive rainfall precipitation events in UDS; node locations refer to Section 3) were selected for model calibration (from April 6, 2018, to April 24, 2018) and model verification (from May 5, 2018 to May 21, 2018). For nodes J5, J35, and J41, their model calibration-averaged Nash–Sutcliffe efficiency (NSE) values were 0.849, 0.862, and 0.874, respectively; their model validation averaged NSE values were 0.843, 0.856, and 0.862, respectively (see detailed information in Table 1, Figure 4 and Figure 5). Figure 6 displays a comparison of the modeled and measured values at node J41 during calibration on April 9, 2018, and verification on May 21, 2018.

2.4.3. Realization of PSO Algorithm Optimization. The decision-making of the abovementioned objective function in this study involved the nonlinear decision-making of discrete variables. The discreteness of variables makes the objective function and constraint function of the problem neither continuous nor differentiable in its feasible set, which makes it difficult to implement analytical methods. Earlier studies suggested that the key advantages of the PSO algorithm include simple structure, few parameters, easy realization in engineering, and suitability in solving the nonlinear discrete variable problem. Its rapid search speed could reduce the computation time of a model [36, 37]. Thus,

Table 1: Nash–Sutcliffe efficiency (NSE) results for verification and calibration of the UDS model on different rainfall events.

Rainfall event		Nash–Sutcliffe efficiency (NSE)		
		Node J5	Node J35	Node J41
Verification	20180406	0.812	0.899	0.849
	20180409	0.832	0.837	0.890
	20180414	0.875	0.834	0.904
	20180415	0.873	0.876	0.862
	20180416	0.853	0.861	0.869
	20180424	0.846	0.862	0.870
Calibration	20180505	0.871	0.891	0.869
	20180507	0.832	0.802	0.842
	20180511	0.874	0.895	0.858
	20180513	0.820	0.831	0.843
	20180515	0.832	0.854	0.851
	20180521	0.833	0.861	0.906

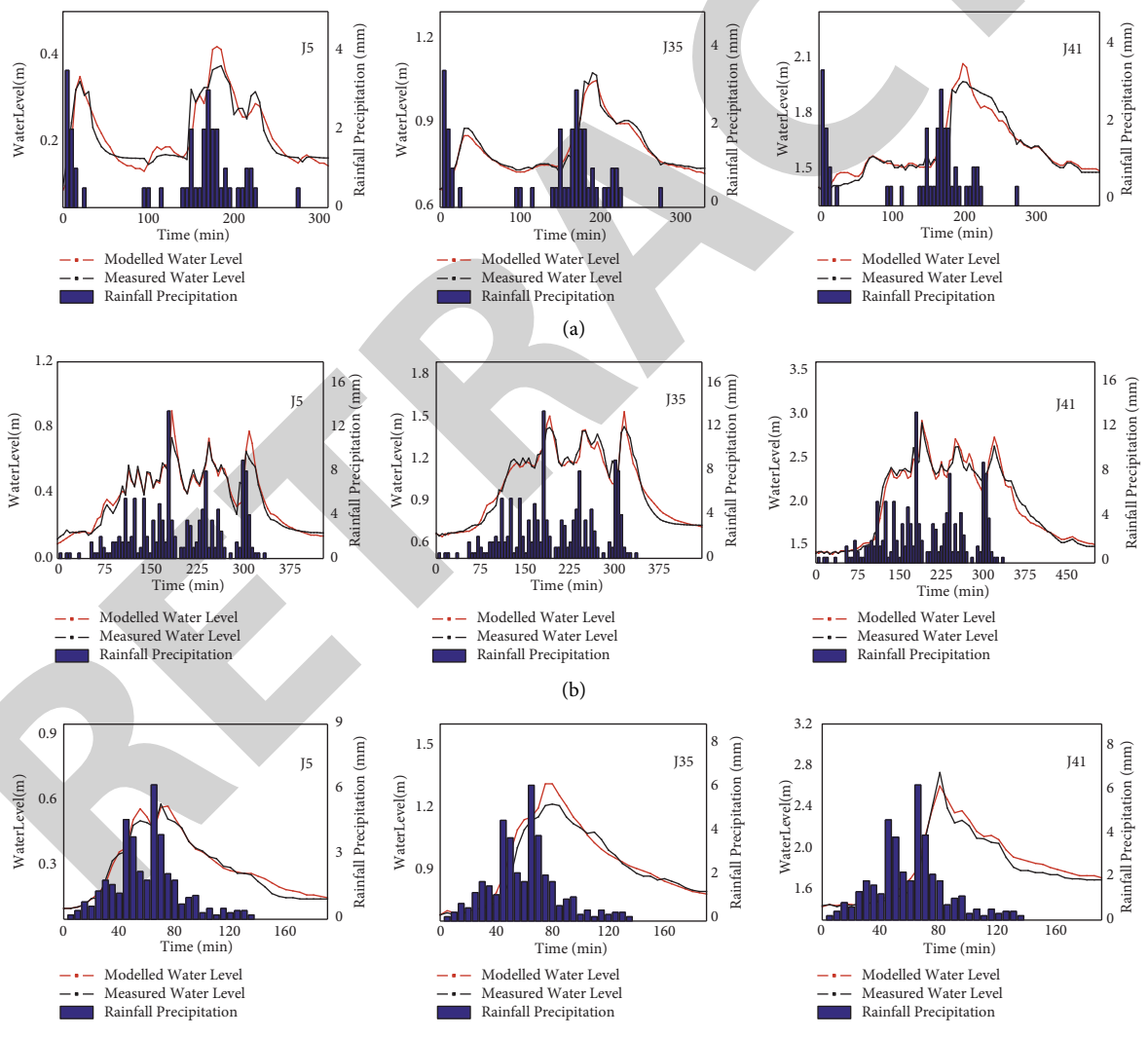

Figure 4: Continued.

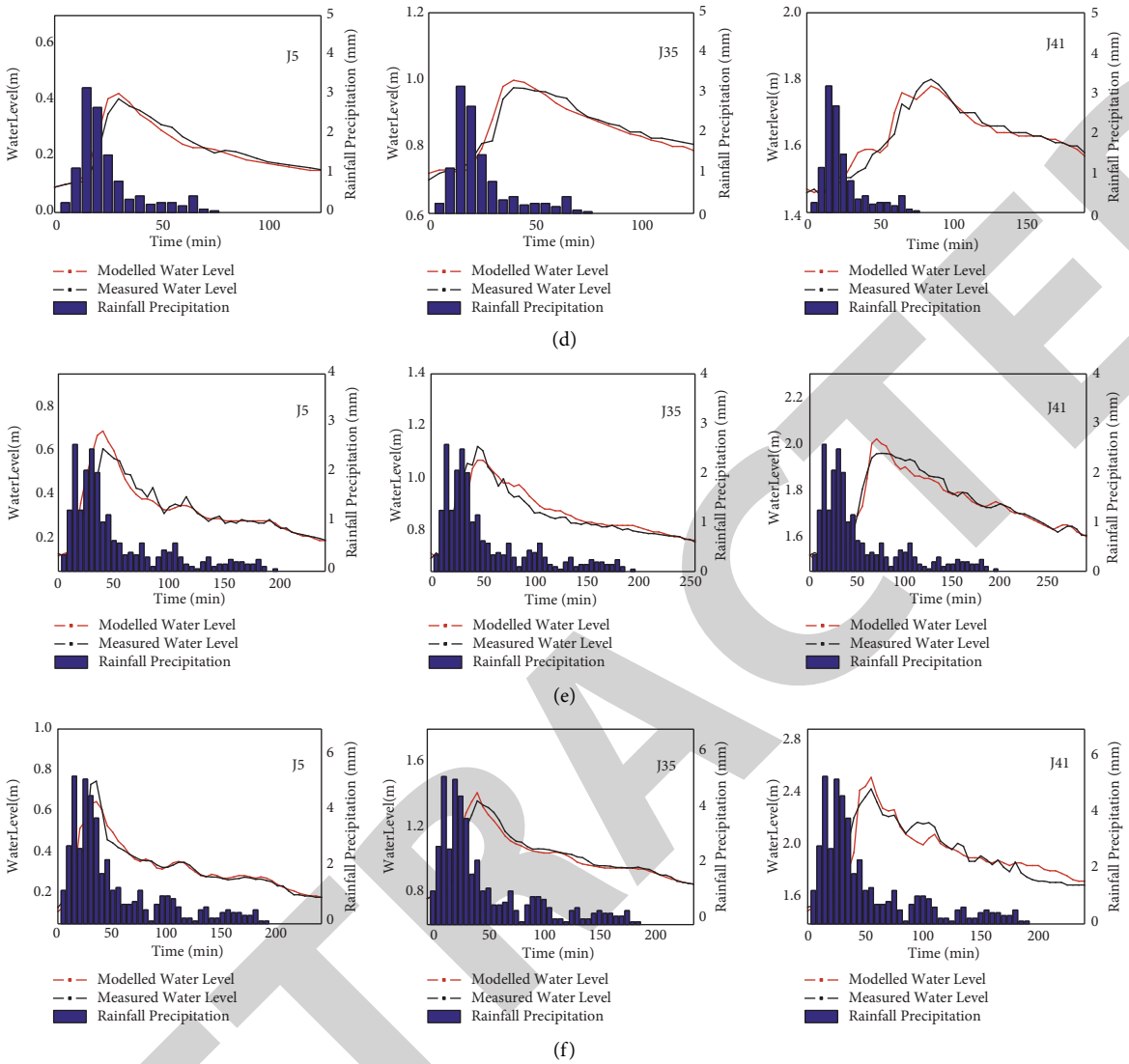

Figure 4: Modeled and measured water-level values for verification of the UDS model on the (a) 20180406, (b) 20180409, (c) 20180414, (d) 20180415, (e) 20180416, and (f) 20180424 rainfall events.

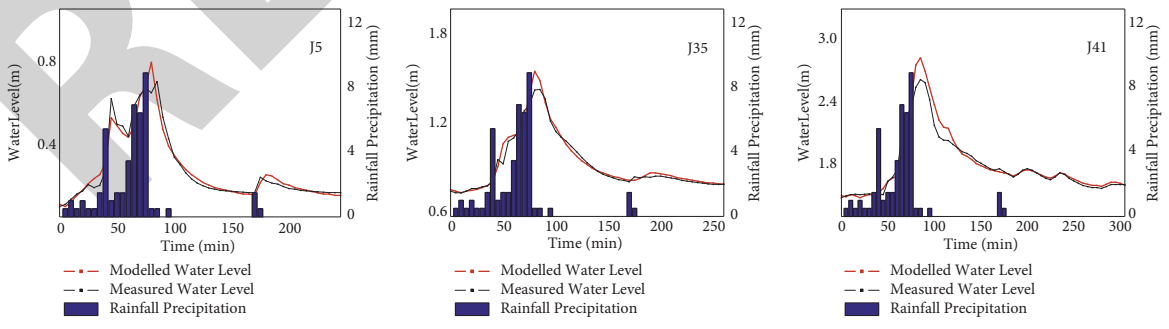

Figure 5: Continued.

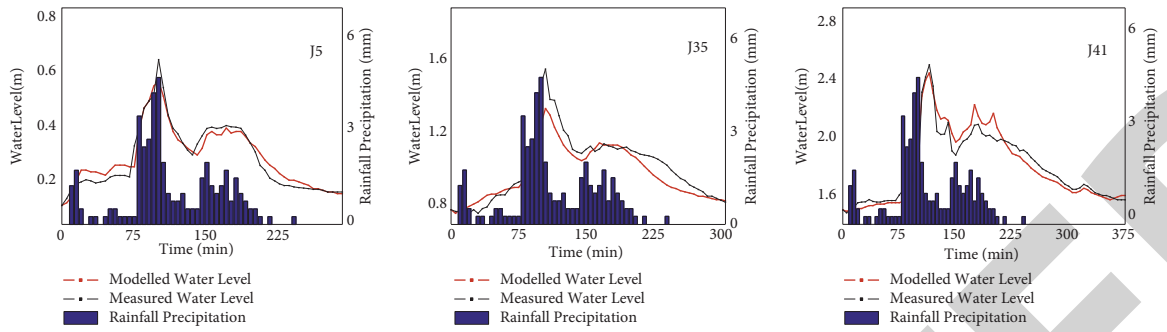

(b)

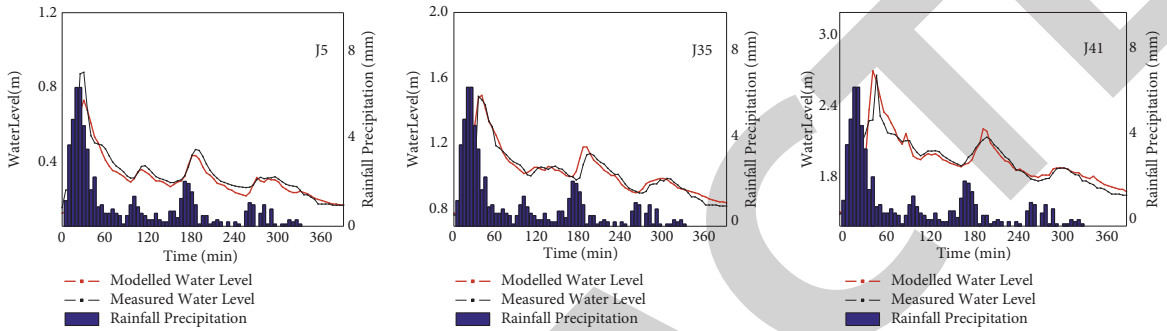

(c)

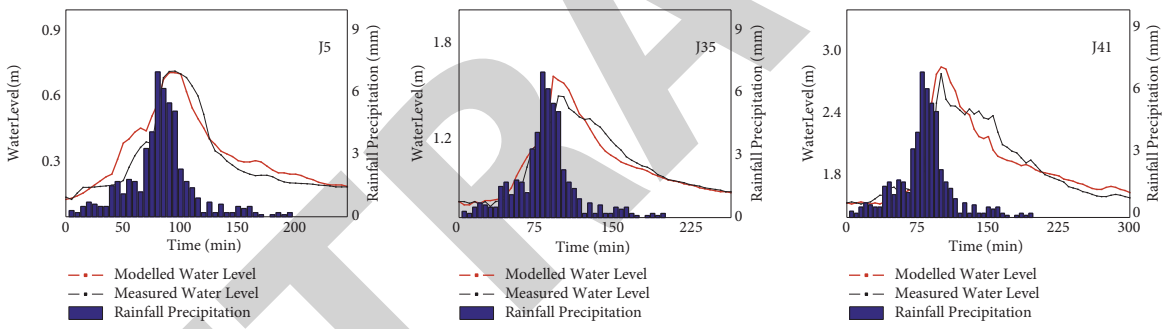

(d)

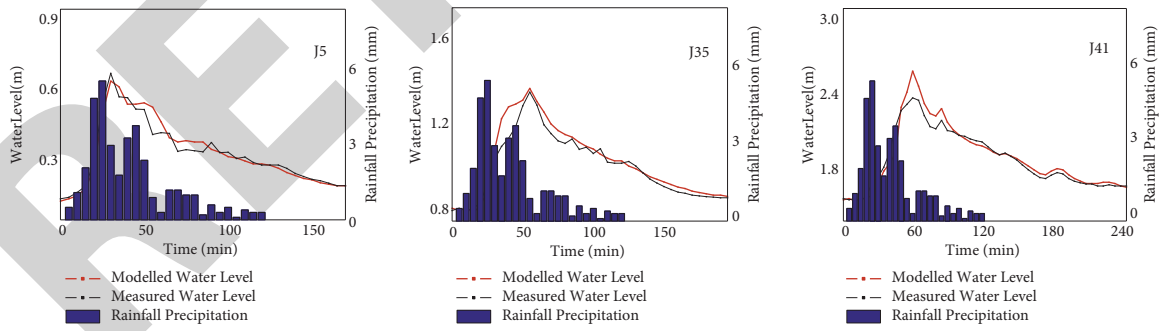

(e)

Figure 5: Continued.

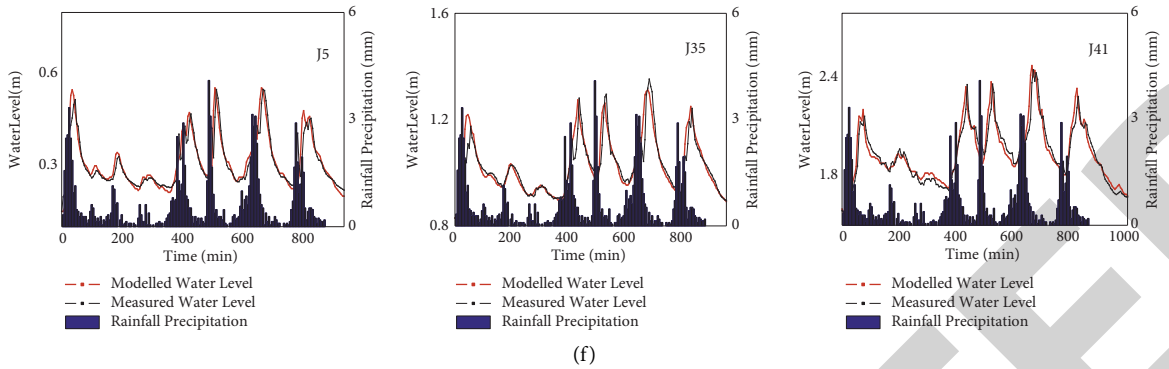

Figure 5: Modeled and measured water-level value for calibration of the UDS model on the (a) 20180505, (b) 20180507, (c) 20180511, (d) 20180513, (e) 20180515, and (f) 20180524 rainfall events.

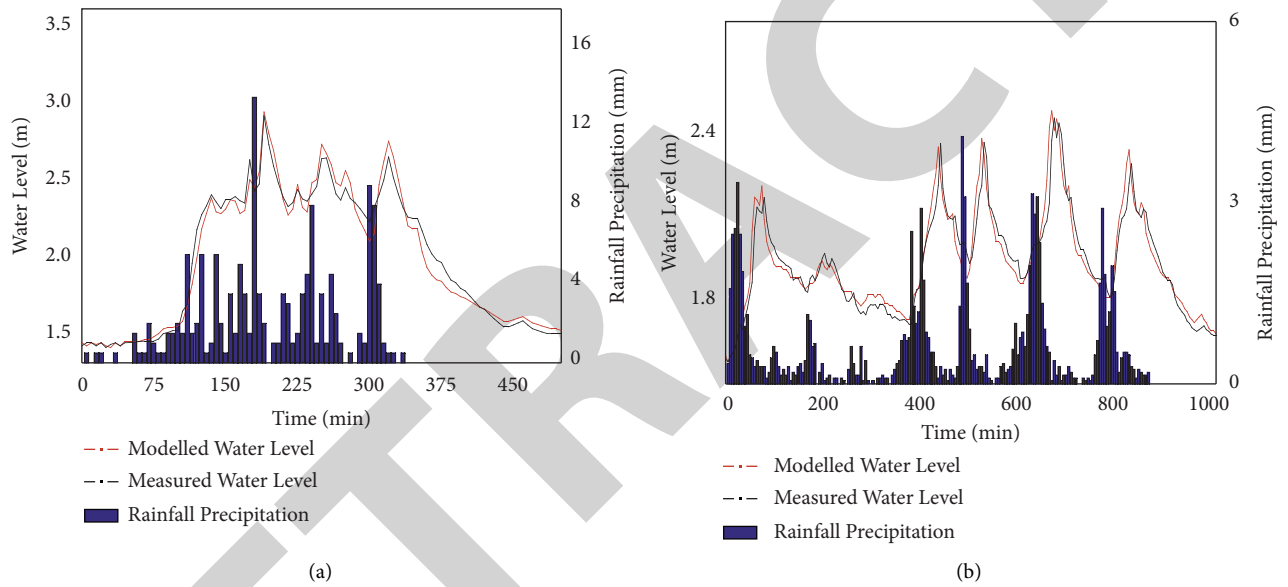

Figure 6: Modeled and measured water level in node J41. Events of (a) 09/04/2018 (NSE = 0.890) and (b) 21/05/2018 (NSE = 0.906).

this algorithm was selected to perform decision optimization in this model. This algorithm first obtained an initial generation of a particle swarm with a random position vector $\overrightarrow{X_1}$ (t) and velocity vector $\overrightarrow{V_1}$ (t). Next, it updated the position and the velocity vectors of the particle swarm through the velocity (4) and position (5) vector formulas. The second generation of iterative particles, called individual extremum, was obtained by comparing the position of particles after the iteration with that before the iteration. The best particle from the second generation of particles was selected as the global extremum. The iteration continued to the end. The fitness function was applied to evaluate the quality of particles. In this study, the computation results of the SWMM model were used as the fitness function to evaluate the quality of the particles. The model adopted the Python library to send control commands, and MatSWMM was used to realize the interaction between the SWMM model and the Python library, which is an open-source toolbox developed by Briceno-Riano et al. [38]. Since NumPy has fast array processing capabilities and its data structures can store and manipulate data more efficiently, the specific type of Python library used in this article is NumPy. The part parameter values of PSO were determined in accordance with a previously reported summary and recommendation [39]. The inertia weight in this model was set as 1, and the personal and global learning constants were set as 2. The maximum and minimum velocity vectors were set as 20 and −20, respectively. The numbers of particle swarms and iterations were obtained from the convergence test of the PSO algorithms. Eventually, the number of particle swarms and iterations in this study were set to 30 (see detailed information in Figure 7). The overall framework of the MPC model is shown in Figure 8.

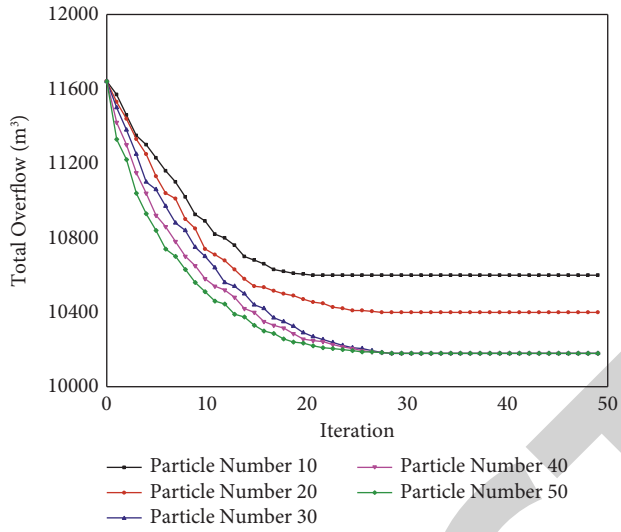

Figure 7: Performance of the PSO algorithm with different particle numbers.

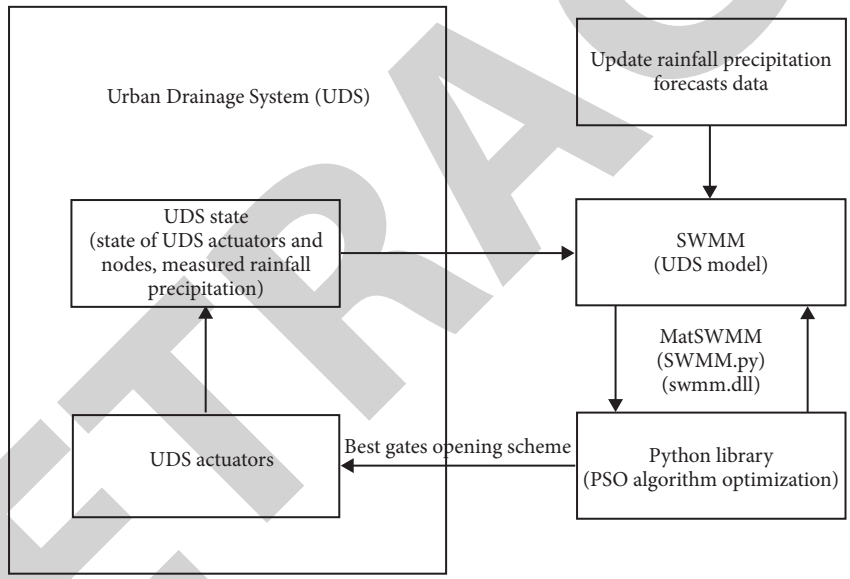

Figure 8: The overall framework of the MPC model.

$$\overrightarrow{V_i}(t+1) = Y(t)\overrightarrow{V_i}(t) + \text{random}[0,1]C_1 \cdot \left(\overrightarrow{p\text{Best}_i}(t) - \overrightarrow{X_i}(t)\right) + \text{random}[0,1]C_2 \cdot \left(\overrightarrow{g\text{Best}_i}(t) - \overrightarrow{X_i}(t)\right), \quad (4)$$

$$\overrightarrow{X_i}(t+1) = \overrightarrow{X_i}(t) + \overrightarrow{V_i}(t+1). \quad (5)$$

In Equations (4) and (5), Y is the inertia weight at iteration t; random$[0, 1]$ is a random number in $[0, 1]$; C_1 and C_2 are personal and global learning constants, respectively; $\overrightarrow{p\text{Best}_i}(t)$ is the best personal experience of the *ith* particle at iteration t; and $\overrightarrow{g\text{Best}_i}(t)$ is the best experience among all particles at iteration t.

2.5. Model-Running Process. In the model-running process, the whole period of the rainfall event $[t_1, t_{\text{end}}]$ was divided into H time periods according to the amount of rainfall. In one of the time periods $[t_1, t_2]$, the precipitation forecasts in time periods $[t_1, t_{\text{end}}]$ and the current UDS situation were input into the model to derive the decision rule R_1. This rule was then used for real-time UDS control. In the new time period $[t_2, t_3]$, the rainfall forecasts in the time period $[t_2, t_{\text{end}}]$ and the current UDS situation were input into the model to derive the decision rule R_2. This rule was also implemented for real-time UDS control. The current UDS situation data were gathered through the field sensors and actuators, including the sensor-observed water level data of the UDS nodes, the rainfall precipitation data, and the gate-opening value in the time period $[t_1, t_2]$. In the new time period $[t_3, t_4]$, the rainfall forecasts in the time period

$[t_3, t_{end}]$ and the current UDS situation were channeled into the model in order to derive the decision rule R_3. Such a rule was further implemented for real-time UDS control. The UDS situation data are the sensor-observed water level data of the UDS nodes, the rainfall precipitation data, and the gate-opening value in the time period $[t_1, t_3]$ gathered through the field sensors and actuators. This process was continued until t_{end}. Hence, R_1, R_2 , . . ., R_H, total H decision rules were utilized for real-time UDS control in the whole rainfall event. Figure 9 shows the timeline of the model-running process. Since the minute-level precipitation forecasts of the National Weather Center in the next two hours were updated at every 6-minute time step, they were adopted as the model precipitation forecasts input in the system (http://radar.tianqi.cn/), the model computational time depends on the MPC system server, with 9.6 minutes for a model run once in this system.

2.6. Evaluation of Decision-Making Validity of the MPC System. The output result of the UDS model was the fitness function of the PSO algorithm, which means that if the UDS model can properly simulate the practical situation of the UDS in the field in the decision-making stage of the MPC system, the decision-making of the algorithm is based on the practical situation of the UDS in the field and the decision-making of the MPC system is reliable. The simulated values of the UDS model in the decision-making stage of the MPC system and the sensor-measured values by the field sensors were compared to examine the decision-making validity of the MPC system. It can be evaluated using (6). From (6), when E_{Des} value exceeded 0.75, the UDS model would adequately simulate the practical situation of the UDS in the field and the decision-making of the MPC system would be reliable. When the E_{Des} value surpassed 0.9, the UDS model would accurately simulate the practical situation of the UDS in the field and the decision-making of the MPC system would be very effective [40].

$$E_{\mathrm{Des}} = 1 - \frac{\sum_{t=1}^{T} \left(L_{\mathrm{Mod}}^{t} - L_{\mathrm{Mea}}^{t}\right)^2}{\sum_{t=1}^{T} \left(L_{\mathrm{Mod}}^{t} - \overline{L}_{\mathrm{Mod}}\right)^2}. \tag{6}$$

In (6), T is the total duration, *min*; t is the *t-th* time period, *min*; L_{Mod}^{t} is the simulated water level value of the UDS model in the *t-th* time period, *meter*; L_{Mea}^{t} is the sensor-measured water-level values in the *t-th* time period, *meter*; and $\overline{L}_{Mod}$ is the average simulation water-level value of the UDS model in the total duration, *meter*.

3. Real Time Monitor and Control System Networks

Real-time monitoring and control system networks are the bases of the MPC system. Real-time monitor and control system includes one rainfall-monitoring station (installed rain gauge), three UDS node water level monitoring stations (installed water level gauge; for J5, J35, and J41 nodes' locations, refer to Figure 10), and a boundary condition monitoring station (installed water level gauge; outside the outfall), and seven actuators stations (seven sluice gates at the study catchment). The data collection interval of sensors was set to 5 minutes in this study. The selection of three UDS node stations was based on Guo et al. [41]. Seven sluice gates are the original actuators of the study catchment. Figure 10 presents the establishment of the real-time monitor and control system networks at the study catchment.

4. Results and Discussion

4.1. Application of the MPC System. In this section, the control effect of the MPC system is evaluated by comparing the flood inundation situation controlled by three control scenarios during three typical rainfall events (i.e., the original control scenario, current MPC, and ideal MPC). The total rainfall of the three rainfall events is similar. The boundary conditions, that is, the water level in the outer river, are in the low, late high, and storm surge tide periods, which are representative of evaluating the application effect of the MPC system. The original control scenario is the real-time control scenario in the studied catchment before the application of MPC. It is a simple binary setting (off and on) based on the water level in front of the gate, determined by practical experience, and the specific control rules are shown in Table 2. The current MPC is a time series of control settings, and the control time step is 10 min with a control horizon of 120 min (the time scale of rainfall forecast data is 120 min, refer to Subsection 2.5), In each time step, it provides 11 possible choices for gate opening (refer to Subsection 2.4) and the model-running processes (refer to Subsection 2.5). The ideal MPC is the result of an MPC whose actual rainfall precipitation is known and actual rainfall precipitation is taken as the model input to get the best control rules [28–30]. Thus, the control rules of an ideal MPC are ideal real-time control rules, and the result of an ideal MPC is mainly used to confirm the application effect of the MPC system in practical applications (the current MPC) in this study. The sensor-measured rainfall precipitation, and tide level data of the three rainfall events are shown in Figure 11.

Table 3 indicates that for the rainfall event on June 24, 2018, the current MPC (ideal MPC) reduced the total overflow by 37.3% (43.1%), cut the total overflow time of nodes to 43.6% (48.9%), and delayed the average time of node overflow start time by approximately 18.1 minutes (20.5 minutes) compared with the original control scenario. For the rainfall event on August 7, 2019, the current MPC (ideal MPC) lowered the total overflow by only 10.8% (12.2%) and total overflow time to 35.4% (39.1%) and dragged the average time of node overflow start time by approximately 9.67 minutes (10.54 minutes) compared with the original control scenario. Although the reduction of the total overflow is limited, the total overflow time is greatly reduced. For the rainfall event on September 16, 2018, the current MPC dropped the total overflow of nodes and total overflow time by 5.4% (6.06%) and 11.4% (12.4%), respectively. Relative to the original control scenario, it

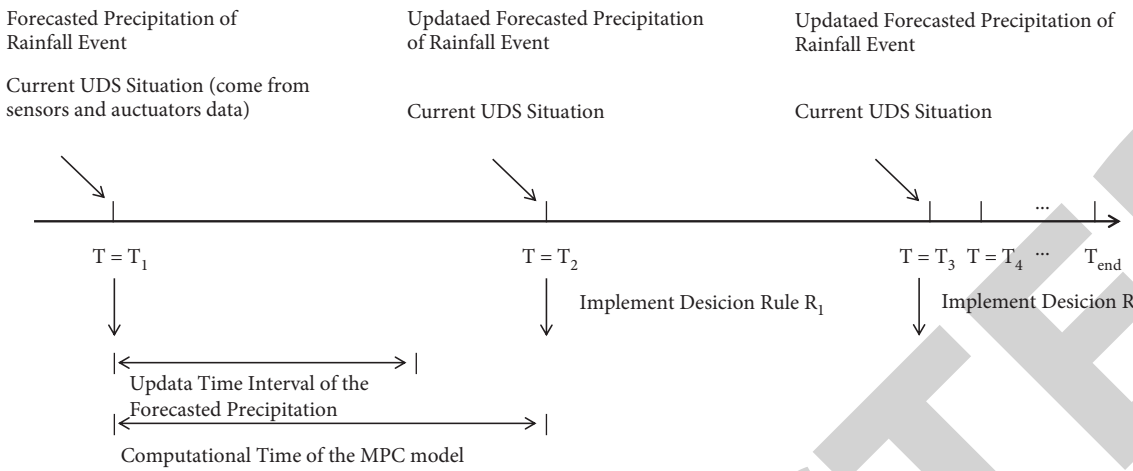

Figure 9: Timeline of the MPC model-running process.

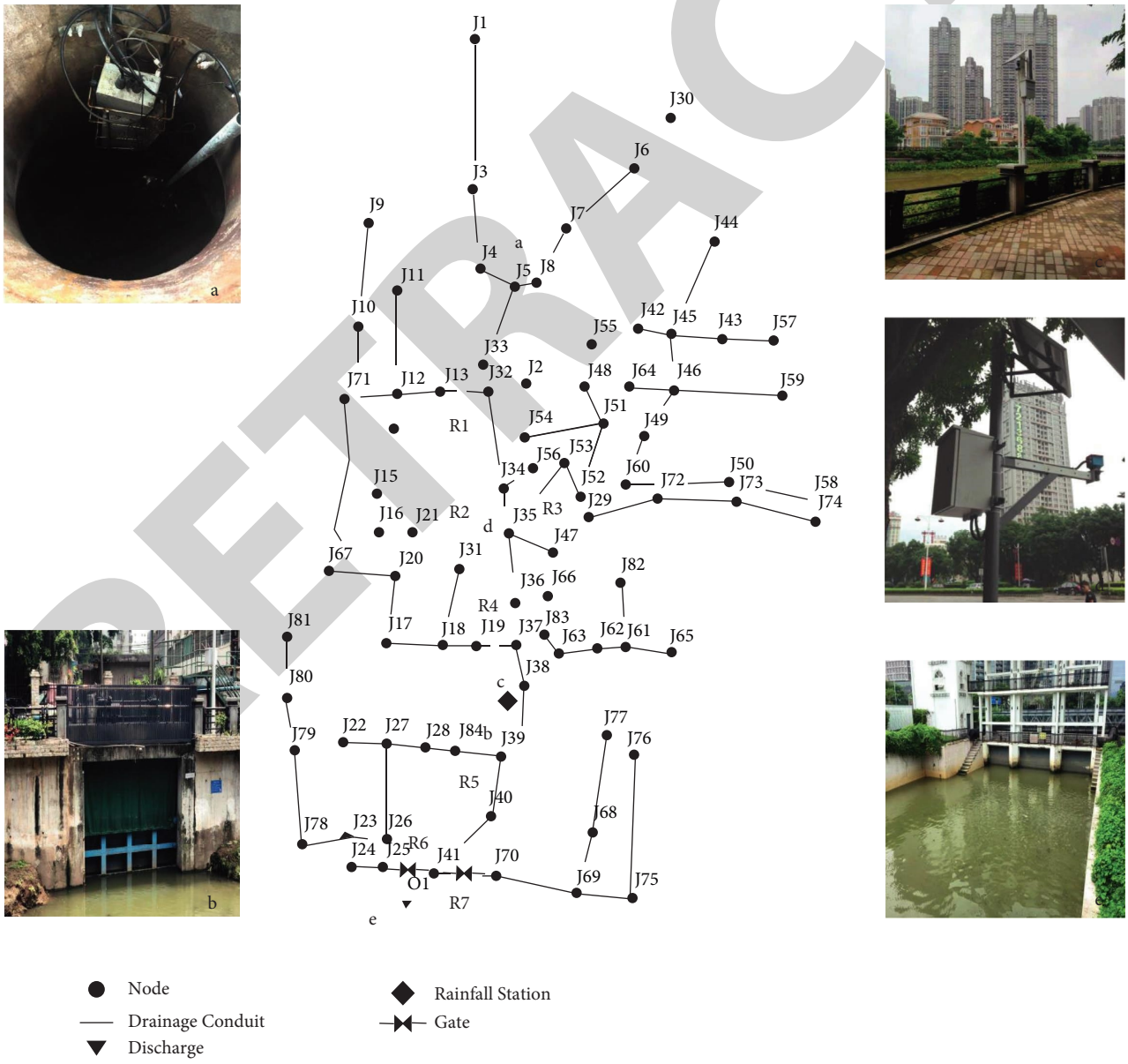

Node
Drainage Conduit
Discharge
Rainfall Station
Gate

Figure 10: Real-time monitor and control system in the field. In the figure, the serial numbers (a), (b), (c), (d), and (e) present sensors and actuators installed in the field, and the serial number R1, R2,...,R7 represents the number of the gates.

Table 2: The control rules of the original control scenario (the location and number of gates are in accordance with Figure 10).

	R1	R2	R3	R4	R5	R6	R7
Gate height (m)	3.0	3.0	2.0	3.0	3.0	2.0	3.0
Gate-on (m)	3.0	2.1	1.8	2.8	3.0	1.2	3.0
Gate-off (m)	1.9	0.9	1.7	2.4	2.5	1.0	2.7

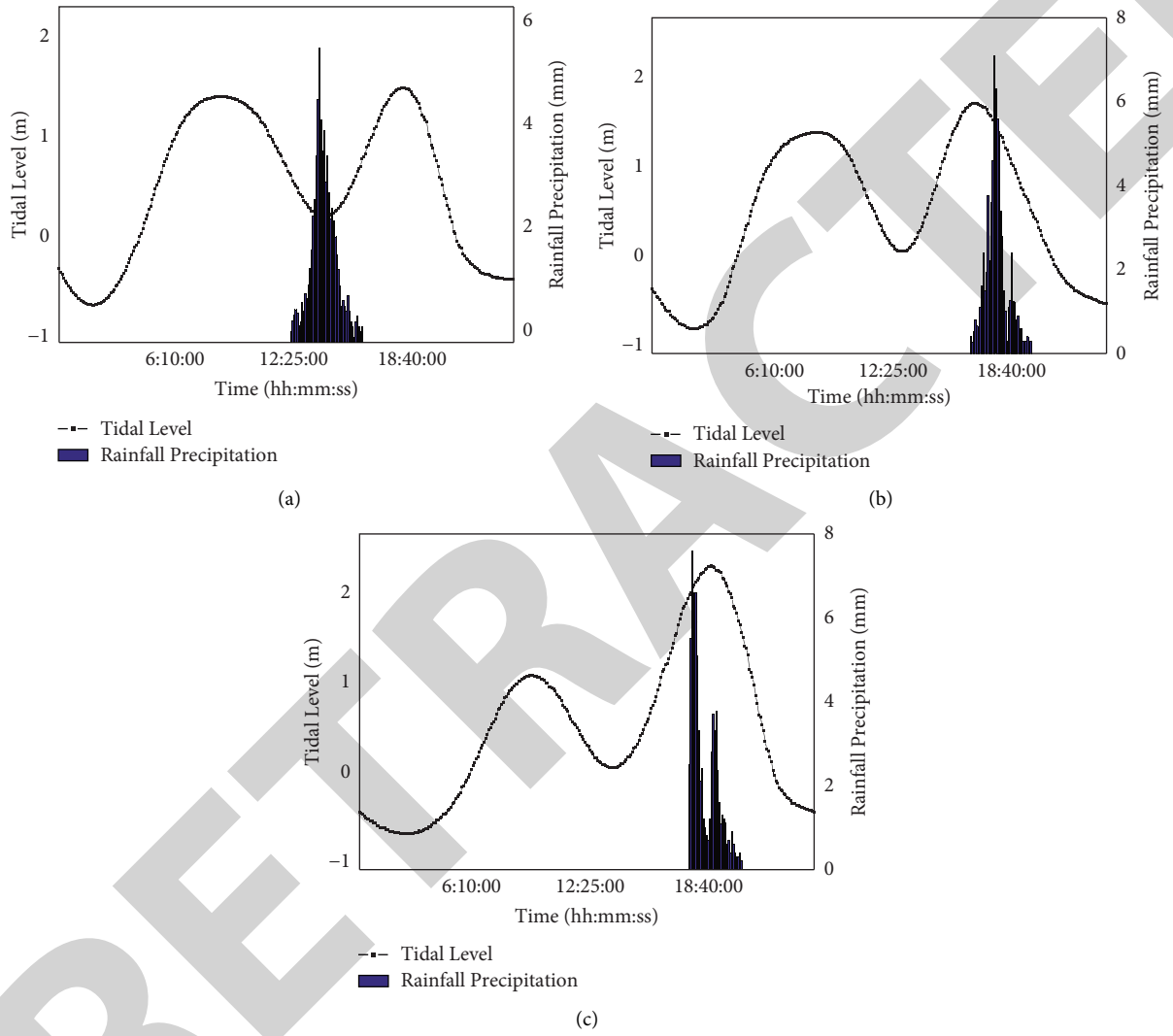

Figure 11: Sensors-measured rainfall precipitation and tide level of the (a) 20180624, (b) 20190807, and (c) 20180916 rainfall events.

Table 3: Results of the original control scenario, the current MPC, and the ideal MPC.

		20180624	20190807	20180916
The original control scenario	Rainfall precipitation (mm)	67.53	67.95	70.43
	Total node overflow (m^3)	4635.4	6972.3	10756.6
	Total node overflow time (min)	94	485	907
	Average time of node overflow start time (hh:mm:ss)	13 : 14 : 25	18 : 24 : 50	18 : 20 : 13
The current MPC	Total node overflow (m^3)	2906.2	6219.3	10175.7
	Total node overflow time (min)	53	313	804
	Average time of node overflow start time (hh:mm:ss)	13 : 32 : 31	18 : 34 : 30	18 : 38 : 56
The ideal MPC	Total node overflow (m^3)	2637.7	6121.7	10104.6
	Total node overflow time (min)	48	295	794
	Average time of node overflow start time (hh:mm:ss)	13 : 34 : 55	18 : 35 : 23	18 : 40 : 11

postponed the average time of node overflow start time by approximately 18.78 minutes (19.97 minutes). Whilst the total overflow flow and total overflow time decrease are limited, the average time of node overflow start time can be delayed to a certain degree, which in turn gains some time for taking feasible measures to prevent flood inundation. The above results show that the MPC system can effectively reduce urban flood risk compared to the original control scenario, and its results are close to those of the ideal MPC. Table 4 and Figure12 indicate that all E_{Des} values are greater than 0.75 and the simulated water levels of the UDS model match well with the sensors-measured values at nodes J5, J35, and J41. Therefore, the UDS model of the MPC system can sufficiently simulate the practical situation of the UDS in the field, and the decision-making of the MPC system is reliable. Therefore, the MPC system is an effective tool for managing urban flood risk in practical application.

4.2. MPC Results under Different Rainfall Return Periods. To further examine the effectiveness of the MPC system, the results of the original control scenario and the ideal MPC under a range of rainfall return periods (e.g., 1, 2, 3, 5, and 10 years) are used. The boundary condition is set at the high tidal level period. The rainstorm intensity for rainfall events design can be estimated using Equation (7). The Chicago approach is adopted to distribute the rainfall amounts [34]. This method recommends generating a hydrograph with a rainstorm with the same average intensity of uniform rainfall and peaking at a selected time, and the humidity conditions before peaking are related to the maximum runoff intensity. The design rainfall duration (t) is 120 minutes, and the rainfall peak coefficient (r) is 0.4 (as recommended by the Guangzhou Municipal Water Bureau in the detailed rules for the implementation of Guangzhou drainage management measures). Figure 13 displays the simulated rainfall process timeline of different rainfall recurrence periods. Regarding the boundary condition, we adopt the tidal level process line of 17 : 00–19 : 00 (provided by the General Urban Drainage Plan of Guangzhou City, and compiled by the Guangzhou Municipal Engineering Design & Research Institute). Figure 14 shows the 1-day average annual tidal-level data of the boundary conditions in the catchment.

$$q = \frac{2424.17\,(1 + 0.553lgP)}{(t + 11.0)^{0.668}}. \tag{7}$$

In (7), q is the rainstorm intensity, $L/s{\cdot}ha$; t is the rainfall duration, min; and P is the design return period, year.

Table 5 indicates that the control effect of the MPC system is gradually limited because of the increase in rainfall return periods. When the catchment encounters rainfall at its 20-year return period, the usage of MPC results barely reduces the total overflow (by 1.23%) and total overflow time (by 1.93%), and delays the average time of node overflow start time by 3.45 minutes compared with the original control scenario. Suppose the control criterion is set to one of the following three criteria: reducing the total overflow by 10%, the total overflow time by 10%, or delaying the average time of node overflow start time by 10 minutes compared with the original control scenario, the results show that the MPC system is only effective when the catchment encounters a rainfall return period of less than three years. Therefore, the MPC system cannot significantly mitigate flood risk in this catchment.

5. Discussion

From Subsections 4.1 and 4.2, we deduce that the MPC system can effectively reduce urban flood risk under different tidal levels for rainfall events with return periods <3 years. However, for rainfall events with return periods >3 years, the effect is limited at the high tidal levels because of the low design capacity of UDS and inadequate maintenance. The effectiveness of the MPC system is closely related to the specific characteristics of a catchment, including the maximum surplus capacity of the UDS, the layout of UDS networks and affiliated gates, and the characteristics of tide level. For a watershed with limited flood risk, suppose it has a suitable layout of UDS networks and a large surplus capacity of UDS, the application of the MPC system for real-time control of UDS in urban flood risk mitigation should be more effective. For instance, Celestini et al. [42] demonstrated that flood inundation could be fully mitigated by simple control rules. Also, AbouRjeily et al. [28] suggested that flood inundation driven by a rainfall event with a return period of 5 years could be alleviated effectively by the real-time UDS control of the MPC system. Nevertheless, for an urban catchment characterized by an unsuitable layout of UDS networks and a low surplus capacity of UDS (usually in developing countries; also the case in the current study), the application effect of the MPC system is rather limited. In practical applications, it is very likely that there will be mismatches, transmission timeouts, or the maximum limit of data after the end is different from the actual transmission bits and misalignments during transmission. In a sense, capital measures and adaptive measures, such as proper expansion and reconstruction of the UDS, control of rainwater runoff in the source (e.g., DT, LID control, and green infrastructure (GI) control measures), are vital for managing urban flood risk in those catchments [11, 43, 44].

However, the MPC system remains important for mitigating urban flood risk because

(i) The MPC system can mitigate urban flood risk. For example, the real-time alert of client software can notify residents about the upcoming urban flood inundation. In this study, the MPC system remains effective when it encounters a rainfall event with a return period of <3 years.

(ii) It provides assistance for capital measures and adaptive measures. Large real-time data (real time rainfall and tide levels) collected by the MPC system can support the implementation of capital measures and adaptive measures, thus saving some implementation cost and time.

Table 4: Decision-making validity of the MPC system.

Decision-making validity value	Rainfall event	UDS node		
		J5	J35	J41
E_{Des}	20180624	0.883	0.849	0.829
	20190807	0.876	0.869	0.871
	20180916	0.870	0.862	0.854

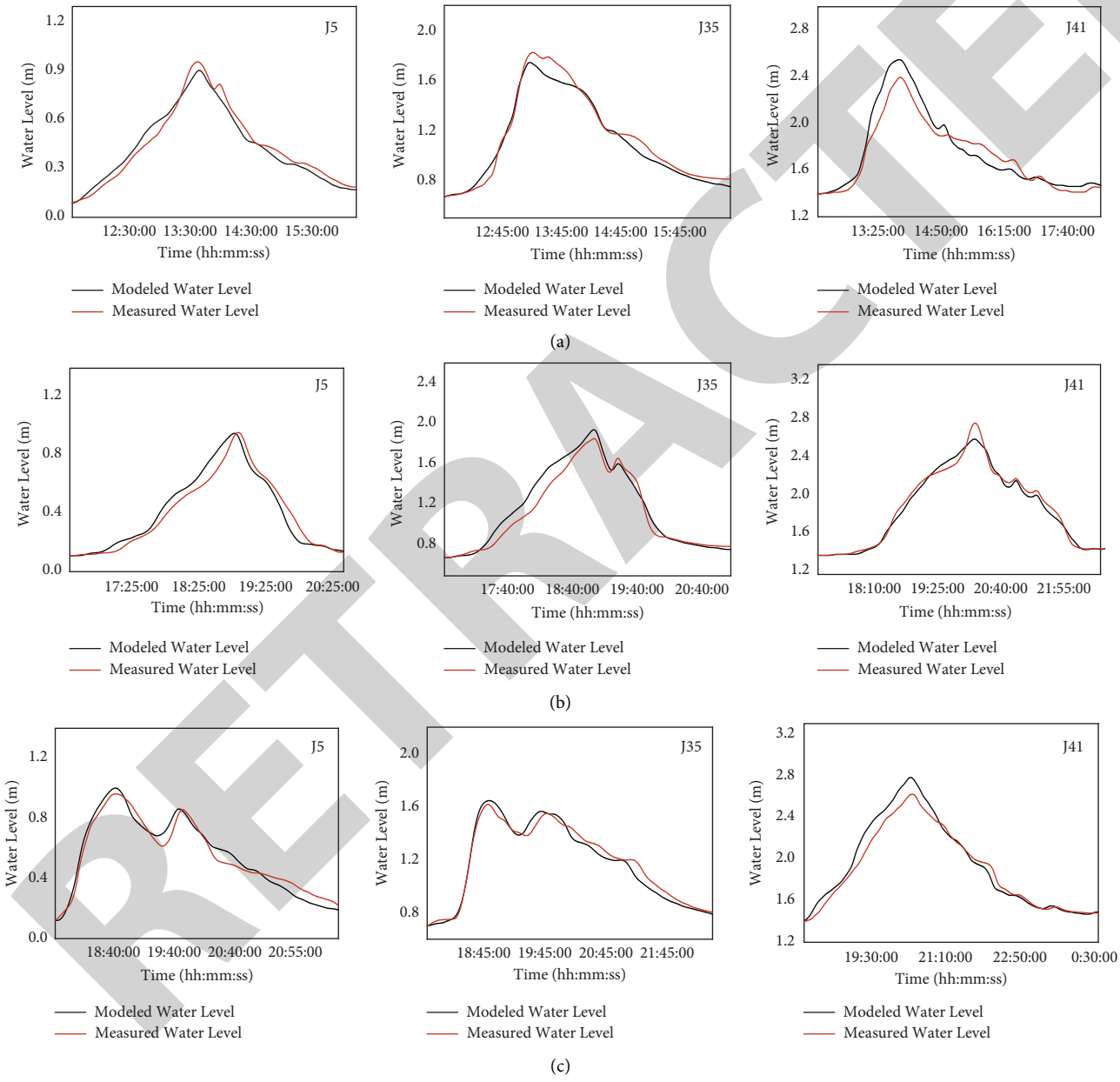

Figure 12: Comparison between simulated water level of UDS model and sensors-measured water level in three nodes on the (a) 20180624, (b) 20190807, and (c) 20180916 rainfall events.

(iii) It improves water resource management of the catchment by combining with other advanced systems (Geographic Information System, Flood Early Warning and Forecasts system).

In future studies, we would explore various ways of combining the MPC system and feasible capital or adaptive measures to tackle urban flood risk. In the context of climate change, the global mean sea level rise would cause the tidal

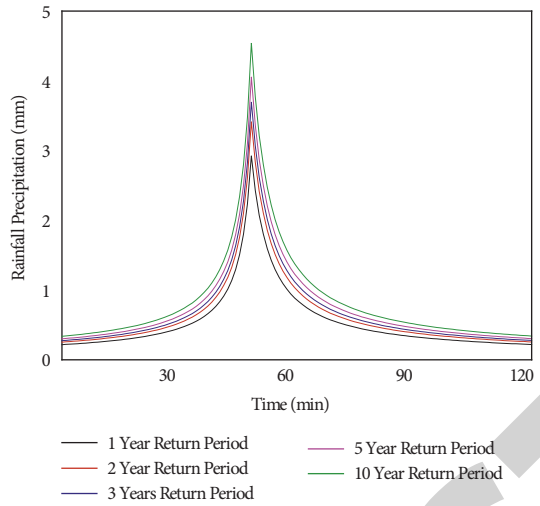

Figure 13: Design rainfall hydrograph under different rainfall return periods.

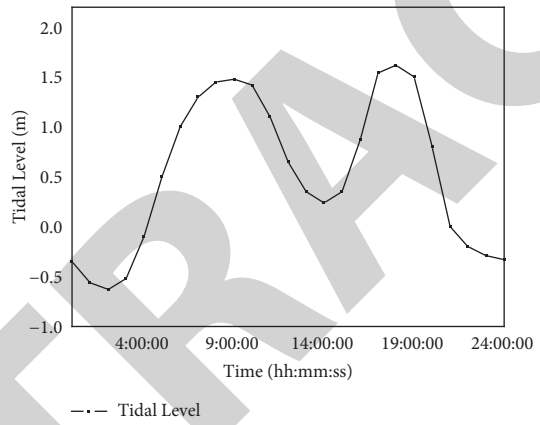

Figure 14: One-day average annual tide level data of boundary constraint conditions.

Table 5: Results of original control scenario and the ideal MPC under different rainfall return periods.

		1-year return period	2-year return period	3-year return period	5-year return period	10-year return period
The original control scenario	Rainfall precipitation (mm)	67.4	78.67	85.23	93.45	104.72
	Total node overflow (m^3)	8,767.3	1,2173.5	19,183.3	27,117.4	43,262.2
	Total node overflow time (min)	824	989	1,125	1,284	1,563
	Average time of node overflow start time (hh:mm:ss)	18 : 25 : 24	18 : 21 : 31	18 : 19 : 03	18 : 12 : 17	18 : 07 : 46
The ideal MPC	Total node overflow (m^3)	8,022.4	11,466.9	18,377.6	26,114	42,730
	Total node overflow time (min)	708	898	1,060	1,227	1,533
	Average time of node overflow start time (hh:mm:ss)	18 : 40 : 41	18 : 34 : 32	18 : 30 : 30	18 : 20 : 40	18 : 11 : 13

level to increase, which might weaken the effectiveness of the MPC system in coastal cities [45]. This effect is not only reflected in the change of drainage time, but also in the submerged outflow state, and the instantaneous flow rate will also be reduced. It is important to explore measures to reduce the impact of sea level rise, and ensure the effectiveness of the MPC system in real-time control of UDS for reducing urban flood risk for these cities. Since Guangzhou is also a coastal city, we plan to rigorously explore this aspect in a future study.

5.1. Uncertainties Analysis. The model uncertainties of the MPC system lie in input data and simulations [30]. Input

data include the precipitation forecasts, updated time of the rainfall precipitation forecasts, time period of the rainfall precipitation forecasts, and real-time sensor data, whereas simulation uncertainty covers the simulation accuracy of the UDS model and the determination of the MPC system server. The simulation accuracy of the UDS model is affected by the underlying surface factors of the study catchment, elevation data, UDS data, and other basic data of the study catchment [46–48]. The MPC system server determines the computation time of the MPC system, affecting the real-time control operation of the MPC system [28]. Thus, the implementation effect of the MPC system for real-time control of UDS in urban flood risk mitigation is affected by various factors. In the application of the MPC system for real-time control of UDS to mitigate urban flood risk, it is the key to control model uncertainties to ensure the final control effect of the MPC system. Any deviation from the above factors might even worsen the final results. In this study, updated rainfall forecast data at every 6-minute time step in the next 2 hours were adopted to reduce data input uncertainties. High-precision basic data of the study catchment were used to establish the UDS model, and real-time sensor data were adopted to adjust the UDS model error in the decision-making stage of the MPC system, ensuring the accuracy of real-time control strategies. Cloud-based computer, configured with the Xeon ® Intel Xeon e5-2699 V5 processors and a total of 32 parallel computing cores, speeds up the computational time of the MPC system by about 9.6 minutes, meeting the recommended requirement of Sadlera et al. [30]. From Subsection 4.1, we can see that the application of the MPC system to real-time control of UDS can mitigate urban flood risk.

Moreover, the uncertainties of system information can significantly affect the application of the MPC system to real-time control of UDS in urban flood risk mitigation. These uncertainties include the uncertainty of rainfall events (e.g., rainfall peak coefficient and distribution of rainfall amount); the uncertainty of boundary conditions (e.g., tidal level); and the uncertainty of drainage system parameters (e.g., the layout of the UDS network, size, slope, and resistance coefficient of drainage conduits) [13, 14]. At a high tidal level, the application effect of the MPC system in the study catchment is limited to a rainfall return period of less than three years (see Subsection 4.2). Therefore, in future work, the uncertainties of system information (i.e., rainfall events, drainage boundary conditions, and drainage system parameters) need to be analyzed and reduced. Especially, the analysis of model uncertainties and system information uncertainties should be integrated into the overall design framework of the MPC system.

6. Conclusions

This study emerged from a lack of understanding about the effectiveness of implementing an MPC system based on the SWMM model and evolutionary algorithms for a real UDS in reducing urban flood risk. Given this knowledge gap, the current study presented a case study of applying an MPC system based on the SWMM model and evolutionary algorithms (involving a functional human interface) to operate UDS gates for the purpose of mitigating flood inundation in a real system in the Liede River catchment, Guangzhou, China. The results showed that the system can effectively mitigate urban flood risk compared to the original control scenario. Examination of the decision-making validity of the MPC system indicated that all E_{Des} values were greater than 0.75; thus, the decision-making of the system was effective. Therefore, the MPC system based on SWMM and evolutionary algorithms to real-time control UDS is an effective tool to mitigate urban flood risk in engineering applications. The analysis of the effect of the MPC system under different rainfall return periods (e.g., 1, 2, 3, 5, and 10 years) suggested that when the tidal level of the outer river is high, the application of the MPC system to real-time control of UDS can effectively mitigate urban flood risk for a rainfall event with a return period of less than three years. Nonetheless, the control effect is rather limited for a rainfall event with a return period of more than three years. In this sense, future work should explore new approaches to combining the MPC system with capital measures or adaptive measures in order to fully address the challenges of urban flooding (e.g., appropriate reconstruction of UDS, DT, and LID control), and whether these approaches could be further adapted in the context of climate change (e.g., mean sea level rise and intense rainfall) for the study catchment.

Data Availability

The data that support the findings of this study are available from the authors with the permission of the Guangzhou Municipal Engineering Design & Research Institute, the Guangzhou Sewage Treatment Co., Ltd, and the Guangzhou Land and Resources Bureau. Restrictions apply to the availability of these data, which were used under license for this study.

Conflicts of Interest

The authors declare no conflicts of interest.

Acknowledgments

This research was funded by Science and Technology Planning Project of Guangdong Province, China (grant number No. 2014A020216006) and Science and Technology Program of Guangzhou, China (grant number 201604020010). The authors thank the support of the Guangzhou Municipal Engineering Design & Research Institute, the Guangzhou Sewage Treatment Co., Ltd., and the Guangzhou Land and Resources Bureau.

References

[1] L. Chang, H. Shen, and F. Chang, "Regional flood inundation nowcast using hybrid SOM and dynamic neural networks," *Journal of Hydrology*, vol. 519, pp. 476–489, 2014.

[2] G. Sezar, K. A. Cevza Melek, B. Ayşenur, and B. Uğur, "Flood modeling of Ayamama river watershed in Istanbul, Turkey," *Journal of Hydrologic Engineering*, vol. 24, Article ID 05018026, 2019.

[3] J. Yazdi, "Improving urban drainage systems resiliency against unexpected Blockages: a Probabilistic approach," *Water Resource Management*, vol. 32, pp. 4561–4573, 2018.

[4] P. S. Kaspersen, N. H. Ravn, K. A. Nielsen, H. Madsen, and M. Drews, "Comparison of the impacts of urban development and climate change on exposing European cities to pluvial flooding," *Hydrology and Earth System Sciences*, vol. 21, pp. 4131–4147, 2017.

[5] Z. W. Kundzewicz, S. Kanae, S. I. Seneviratne, J. Handmer, N. Nicholls, and P. Peduzzi, "Flood risk and climate change: global and regional perspectives," *Hydrological Sciences Journal*, vol. 59, no. 1, pp. 1–28, 2014.

[6] B. K. Mishra, E. A. Rafiei, Y. Masago, P. Kumar, R. K. Regmi, and K. Fukush, "Assessment of future flood inundations under climate and land use change scenarios in the Ciliwung River Basin, Jakarta," *Journal of Flood Risk Management*, vol. 11, pp. 1105–1115, 2018.

[7] M. Tavakoli, F. De Smedt, T. Vansteenkiste, and P. Willems, "Impact of climate change and urban development on extreme flows in the Grote Nete watershed, Belgium," *Natural Hazards*, vol. 71, pp. 2127–2142, 2014.

[8] W. Barreto, Z. Vojinovic, R. Price, and D. Solomatine, "Multiobjective evolutionary approach to rehabilitation of urban drainage systems," *Journal of Water Resources Planning and Management*, vol. 136, pp. 547–554, 2011.

[9] T. C. Walsh, C. A. Pomeroy, and S. J. Burian, "Hydrologic modeling analysis of a passive, residential rainwater harvesting program in an urbanized, semi-arid watershed," *Journal of Hydrology*, vol. 508, pp. 240–253, 2014.

[10] Z. Zahmatkesh, S. J. Burian, M. Karamouz, H. Tavakol-Davani, and E. Goharian, "Low-impact development practices to mitigate climate change effects on urban stormwater runoff: case study of New York city," *Journal of Irrigation and Drainage Engineering*, vol. 141, Article ID 04014043, 2015.

[11] P. Koudelak and S. West, "Sewerage network modelling in Latvia, use of InfoWorks CS and storm water management model 5 in Liepaja city," *Water and Environment Journal*, vol. 22, pp. 81–87, 2008.

[12] J. Yazdi, E. H. Lee, and J. H. Kim, "Stochastic multiobjective optimization model for urban drainage network rehabilitation," *Journal of Water Resources Planning and Management*, vol. 141, Article ID 04014091, 2015.

[13] H. F. Duan, F. Li, and T. Tao, "Multi-objective optimal design of detention tanks in the urban stormwater drainage system: uncertainty and sensitivity analysis," *Water Resources Management*, vol. 30, pp. 2213–2226, 2016.

[14] H. F. Duan, F. Li, and H. Yan, "Multi-objective optimal design of detention tanks in the urban stormwater drainage system: LID implementation and analysis," *Water Resources Management*, vol. 30, pp. 4635–4648, 2016.

[15] F. Li, H. F. Duan, H. Yan, and T. Tao, "Multi-objective optimal design of detention tanks in the urban stormwater drainage system: framework development and case study," *Water Resources Management*, vol. 29, pp. 2125–2137, 2015.

[16] F. Li, Y. Xufeng, and H. F. Duan, "Sustainable design of urban stormwater drainage systems by implementing detention tank and lid measures for flooding risk control and water quality management," *Water Resources Management*, vol. 33, pp. 3271–3288, 2019.

[17] H. F. Duan and X. Gao, "Flooding control and hydro-energy assessment for urban stormwater drainage systems under climate change," *Water Resources Management*, vol. 33, pp. 3523–3545, 2019.

[18] S. Hellmers, N. Manojlovic´, G. Palmaricciotti, S. Kurzbach, and P. Fröhle, "Multiple linked sustainable drainage systems in hydrological modelling for urban drainage and flood risk management," 2015, https://www.google.com/search?q=Multiple+linked+sustainable+drainage+systems+in+hydrological+modelling+for+urban+drainage+and+flood+risk+-management&rlz=1C1GCEB_enIN993IN993&oq=Multiple+linked+sustainable+drainage+systems+in+hydrological+modelling+for+urban+drainage+and+flood+risk+management&aqs=chrome.0.69i59j69i60.61218j0j4&sourceid=chrome&ie=UTF-8.

[19] F. Babovic and A. Mijic, "The development of adaptation pathways for the long term planning of urban drainage systems," 2019, https://onlinelibrary.wiley.com/doi/abs/10.1111/jfr3.12538.

[20] L. Garcíaa, J. Barreiro-Gomez, E. Escobar, D. Télleza, N. Quijanoa, and C. Ocampo-Martinez, "Modeling and real-time control of urban drainage systems: a review," *Advances in Water Resources*, vol. 85, pp. 120–132, 2015.

[21] M. S. Gelormino and N. L. Ricker, "Model-predictive control of a combined sewer system," *International Journal of Control*, vol. 59, pp. 793–816, 1994.

[22] S. Heusch and M. Ostrowski, "Model predictive control with SWMM," *Journal of Water Management Modeling*, vol. 19, pp. 237–247, 2011.

[23] N. S. V. Lund, A. K. V. Falk, M. Borup, H. Madsen, and P. S. Mikkelsen, "Model predictive control of urban drainage systems: a review and perspective towards smart real-time water management," *Critical Reviews in Environmental Control*, vol. 48, pp. 279–339, 2018.

[24] A. L. Mollerup, P. S. Mikkelsen, D. Thornberg, and G. Sin, "Controlling sewer systems – a critical review based on systems in three EU cities," *Urban Water Journal*, vol. 14, pp. 435–442, 2017.

[25] J. Lemos and L. Pinto, "Distributed linear-quadratic control of serially chained systems: application to a water delivery canal," *IEEE Control Systems*, vol. 32, pp. 26–38, 2012.

[26] M. Marinaki and M. Papageorgiou, "Linear-quadratic regulators applied to sewer network flow control," in *Proceedings of the European Control Conference*Cambridge, United Kingdom, 2003.

[27] P. K. Rai, C. T. Dhanya, and B. R. Chahar, "Flood control in an urban drainage system using a linear controller," *Water Practice and Technology*, vol. 12, pp. 942–952, 2017.

[28] Y. AbouRjeily, O. Abbas, M. Sadek, I. Shahrour, and C. F. Husseinhage, "Model predictive control for optimising the operation of urban drainage systems," *Journal of Hydrology*, vol. 566, pp. 558–565, 2018.

[29] F. Jafari, J. Mousavi, J. Yazdi, and J. H. Kim, "Real-time operation of pumping systems for urban flood mitigation: Single-period vs. Multi-period optimization," *Water Resources Management*, vol. 32, pp. 4643–4660, 2018.

[30] J. M. Sadler, J. L. Goodall, M. Behl, M. M. Morsy, and B. D. Bowes, "Leveraging open source software and parallel computing for model predictive control of urban drainage systems using EPA-SWMM5," *Environmental Modelling & Software*, vol. 120, pp. 1–13, 2019.

[31] H. Yu, Y. Zhao, Y. Fu, and L. Li, "Spatiotemporal variance assessment of urban rainstorm waterlogging affected by

impervious surface expansion: a case study of Guangzhou, China," *Sustainability*, vol. 10, p. 3761, 2018.

[32] H. Yu, Y. Zhao, and Y. Fu, "Optimization of impervious surface Space layout for prevention of urban rainstorm waterlogging: a case study of Guangzhou, China," *International Journal of Environmental Research and Public Health*, vol. 16, p. 3613, 2019.

[33] W. Du, N. Chen, S. Yuan, C. Wang, M. Huang, and H. Shen, "Sensor web-Enabled flood event process detection and instant service," *Environmental Modelling & Software*, vol. 117, pp. 29–42, 2019.

[34] W. Chen, G. Huang, H. Zhang, and W. Wang, "Urban inundation response to rainstorm patterns with a coupled hydrodynamic model: a case study in Haidian Island, China," *Journal of Hydrology*, vol. 564, pp. 1022–1035, 2018.

[35] G. Krebs, T. Kokkonen, M. Valtanen, H. Koivusalo, and H. Setälä, "A high resolution application of a stormwater management model (SWMM) using genetic parameter optimization," *Urban Water Journal*, vol. 10, pp. 394–410, 2013.

[36] G. Cavazzini, G. Pavesi, and G. Ardizzon, "A novel two-swarm based PSO search strategy for optimal short-term hydro-thermal generation scheduling," *Energy Conversion and Management*, vol. 164, pp. 460–481, 2018.

[37] J. Yazdi, A. Sadollah, E. H. Lee, D. G. Yoo, and J. H. Kim, "Application of multi-objective evolutionary algorithms for the rehabilitation of storm sewer pipe networks," *Journal of Flood Risk Management*, vol. 10, pp. 326–338, 2018.

[38] G. Briceno-Riano, J. Barreiro-Gomez, A. Ramirez-Jaime, N. Quijano, and C. Ocampo-Martine, "MatSWMM- an open-source toolbox for designing real-time control of urban drainage systems," *Environmental Modelling & Software*, vol. 83, pp. 120–132, 2016.

[39] R. Susuki, F. Kawai, C. Nakazawa, T. Matsui, and E. Aiyoshi, "Parameter optimization of model predictive control using PSO," 2008, https://ieeexplore.ieee.org/document/4654987.

[40] D. N. Moriasi, J. G. Arnold, M. W. V. Liew, R. L. Bingner, R. D. Harmel, and T. L. Veith, "Model evaluation guidelines for systematic quantification of accuracy in watershed simulations," *Transactions of the ASABE*, vol. 50, pp. 885–900, 2007.

[41] X. Guo, M. Li, D. Zhao, and P. Du, "Research and Progress on Optimal Layout of Monitoring Points in Urban Drainage Networks," *China Water & Wastewater*, vol. 4, pp. 26–31, 2018.

[42] R. Celestini, G. Silvagni, and F. Volpi, "The development of integrated real time control to optimise storm water management for the combined sewer system of Rome," *WIT Transactions on The Built Environment*, vol. 139, pp. 317–327, 2014.

[43] H. Jia, H. Yao, Y. Tang, S. L. Yu, R. Field, and A. N. Tafuri, "LID-BMPs planning for urban runoff control and the case study in China," *Journal of Environmental Management*, vol. 149, pp. 65–76, 2015.

[44] A. R. Mcfarland, L. Larsen, K. Yeshitela, A. N. Engida, and N. G. Love, "Guide for using green infrastructure in urban environments for stormwater management," *Environmental Science: Water Research & Technology*, vol. 5, pp. 643–659, 2019.

[45] J. M. Sadlera, J. L. Goodalla, M. Behla, B. D. Bowes, and M. M. Morsyc, "Exploring real-time control of stormwater systems for mitigating flood risk due to sea level rise," *Journal of Hydrology*, vol. 583, 2020.

[46] R. B. Ambrose and T. O. Barnwell, "Environmental software at the U.S. Environmental Protection Agency's center for Exposure assessment modeling," *Environmental Software*, vol. 4, pp. 76–93, 1989.

[47] C. B. S. Dotto, M. Kleidorfer, A. Deletic, W. Rauch, and D. T. McCarthy, "Impacts of measured data uncertainty on urban stormwater models," *Journal of Hydrology*, vol. 508, pp. 28–42, 2014.

[48] S. J. Noh, S. Lee, H. An, K. Kawaike, and H. Nakagawa, "Ensemble urban flood simulation in comparison with laboratory-scale experiments: impact of interaction models for manhole, sewer pipe,and surface flow," *Advances in Water Resources*, vol. 97, pp. 25–37, 2016.